The Temporal Dynamics of Poststroke Neuroinflammation: A Longitudinal Diffusion Tensor Imaging–Guided PET Study with ^{11}C-PK11195 in Acute Subcortical Stroke

Alexander Thiel[1–3], Basia A. Radlinska[2,3], Caroline Paquette[2,3], Michael Sidel[1,2], Jean-Paul Soucy[1,4], Ralf Schirrmacher[1,3,4], and Jeffrey Minuk[1,2]

[1]Department of Neurology and Neurosurgery, McGill University, Montreal, Quebec, Canada; [2]Jewish General Hospital, Montreal, Quebec, Canada; [3]Lady Davis Institute for Medical Research, Montreal, Quebec, Canada; and [4]Brain Imaging Centre, Montreal Neurological Institute, Montreal, Quebec, Canada

Animal experiments suggest that 2 different types of activated microglia (AMG) cells occur in the brain after a stroke: local AMG in the area of the infarct and remote AMG, which occurs along affected fiber tracts. We used ^{11}C-PK11195 PET to image AMG in vivo after stroke in humans in a prospective longitudinal study to investigate the temporal dynamics of AMG and relate local and remote AMG activity to pyramidal tract (PT) damage using diffusion tensor imaging (DTI). **Methods:** Eighteen patients underwent DTI–MRI, ^{11}C-PK11195 PET, and behavioral testing within 2 wk and 6 mo of acute subcortical stroke. In 12 patients, the PT was affected by the stroke (PT group), and in 6 patients it was not (non-PT group). Standardized volumes of interest (VOIs) were placed along the PT at the level of the brain stem, semioval center, and infarct. Tracer uptake ratios (ipsilateral to contralateral) were calculated for each VOI and related to tract damage (measured as fractional anisotropy ratio) and clinical outcome. Six controls underwent the same protocol but only once. **Results:** In both patient groups, local AMG activity in the infarct was increased initially and significantly decreased over the follow-up period. In contrast, remote AMG was detected only in the PT group in the brain stem along the affected tract and persisted during follow-up. No AMG was observed retrograde to the lesion at any time. Remote AMG activity along the affected PT in the brain stem correlated with initial PT damage as measured by DTI in the same tract portion. Local AMG activity in the infarct correlated with anterograde PT damage only at follow-up. After controlling for PT damage, initial AMG activity in the brain stem showed a positive correlation with clinical outcome, whereas persisting AMG activity in the infarct tended to be negatively correlated. **Conclusion:** DTI-guided ^{11}C-PK11195 PET in acute subcortical stroke demonstrates differential temporal dynamics of local and remote AMG. Activity of both types related to anterograde PT damage as measured by DTI and might contribute differently to clinical outcome.

Received Feb. 23, 2010; revision accepted Jun. 17, 2010.
For correspondence or reprints contact: Alexander Thiel, Jewish General Hospital, 3755 Cote St. Catherine Rd., Montreal, QC, Canada, H3T1E2.
E-mail: alexander.thiel@mcgill.ca

Key Words: stroke; inflammation; microglia; recovery; fiber tracts

J Nucl Med 2010; 51:1404–1412
DOI: 10.2967/jnumed.110.076612

Neuroinflammation is a complex acute and chronic reaction of the central nervous system to focal brain lesions (the biologic purpose of which is still the subject of debate) (*1*). One cellular component of neuroinflammation comprises activation of microglia, which are the resident macrophages of the central nervous system (*2*).

In ischemic stroke, inflammatory changes are seen not only in the immediate surroundings of the infarct itself but also in the remote brain regions that have fiber tract connections with the affected area (*3*). Microglia that become active locally, in and around the infarct, have immunohistochemical properties different from microglia activated in remote brain regions (*4*). Locally activated microglia (AMG) consist mainly of cells expressing major histocompatibility complex class I antigens, which are thought to act primarily as scavenger cells (*5*). The role of remote AMG, which predominantly express major histocompatibility complex class II antigens (*6*), is less well understood. It has been hypothesized that these cells may also play a scavenger role by removing degenerating axonal debris and might thus be a histologic correlate of Wallerian (anterograde) degeneration (*7*).

Once activated, microglial cells express a cholesterol transporter protein (TSPO), which was formerly known as peripheral type benzodiazepine receptor, at their outer mitochondrial membrane (*8,9*). PK11195 is a ligand (*10*) that binds to TSPO and, when labeled with the positron-emitting isotope ^{11}C, can be used to image AMG in the brain in vivo. In recent years, ^{11}C-PK11195 has been used

repeatedly to map AMG in various neurologic diseases. In a recent cross-sectional study, we demonstrated that local and remote AMG can be imaged in acute subcortical stroke. We showed that remote AMG is specific to the damaged pyramidal tract (PT) anterograde to the infarct (*11*).

In this paper, we present longitudinal data on the temporal development of AMG over a 6-mo period in patients with a first acute subcortical stroke and relate AMG activity to diffusion tensor imaging (DTI) parameters of fiber tract integrity and clinical outcome. DTI acquires information about the anisotropic diffusion of water molecules along white matter fiber tracts and provides details about tissue microstructure. Fractional anisotropy (FA) provides an index of the diffusion characteristics of water molecules preferentially directed along the axis of major axonal pathways. Changes in FA have been shown to reflect damage to the PT in patients with internal capsule stroke (*12*). Reduced FA has traditionally been interpreted as evidence of Wallerian degeneration and axonal loss after stroke (*13*).

In our study, we specifically addressed whether, in human stroke patients, changes in AMG activity over time were similar for local and remote AMG, degree of local and remote activity related to the extent of fiber tract damage, and initial local and remote AMG activity related to outcome, independent of permanent tract damage.

MATERIALS AND Methods

Patients

Eighteen right-handed patients (13 women, 5 men; mean age ± SD, 73.06 ± 12.99 y) were recruited, assessed, and scanned within 3 wk of a first-ever subcortical stroke and at 6 mo (Table 1). The control group consisted of 6 patients with transient ischemic attack (TIA) (2 women, 4 men) and no structural lesion on the MR image. The PT group consisted of 12 patients (8 women, 4 men) with subcortical ischemic infarction affecting the PT as determined on T1-weighted MRI (7 internal capsule, 3 basal ganglia, and 2 semioval center). Two patients were lost to follow-up. The non-PT group consisted of 6 patients (5 women, 1 man) with subcortical ischemic infarction outside the PT. All groups were similar with respect to age and cardiovascular risk factors. All participants were recruited from the specialized Stroke Unit at the Jewish General Hospital in Montreal, Canada. The study protocol was approved by the McGill University Institutional Review Board, and written informed consent was obtained from all participants.

Behavioral Testing

All patients were assessed for clinical stroke severity and were physically and neurologically examined in the acute poststroke phase. Stroke-related neurologic disability was evaluated using the National Institutes of Health Stroke Scale, and performance in the activities of daily living was assessed using the Barthel Index. The degree of handicap was assessed with the modified Rankin scale, and upper

TABLE 1. Mean Values ± SD of Age, Infarct Volume, RMFT Scores, and R_{FA} of Entire Pyramidal Tract and Tract Portions

			Median time to imaging			Initial					Follow-up				
Group	*n*	Age (y)	Days	Range	Infarct volume (mm^3)	RMFT	R_{FA} total	R_{FA} below	R_{FA} above	RMFT	R_{FA} total	R_{FA} below	R_{FA} above
PT	12/10	76.0 ± 12.33	9	10	5,484 ± 8,557.4	9.3 ± 5.12	0.93* ± 0.060	0.95* ± 0.047	0.96* ± 0.074	10.5 ± 5.11	0.90* ± 0.110	0.89* ± 0.110	0.95* ± 0.106
Non-PT	6	67. ± 13.3	6.5	18	1184 ± 628.3	13.7 ± 1.51	1.023 ± 0.041	0.99 ± 0.041	1.01 ± 0.076	14.3 ± 0.82	1.021 ± 0.030	0.97 ± 0.039	1.05 ± 0.045
Control	6	65.1 ± 6.18	—		—	15.0 ± 0.00	1.018 ± 0.029	—	—	—	—	—	—

*R_{FA} are lower for PT group than for non-PT and control groups (2-way repeated-measures ANOVA, $P < 0.01$) but are unchanged over time.

limb motor function was assessed with the arm subsection (*14*) of the Rivermead Motor Function Test (RMFT) (Table 1).

MRI

T1-weighted (1-mm isotropic voxels; spoiled gradient-echo sequence; repetition time, 9.7 ms; echo time, 4 ms; and α, 12°) and diffusion-weighted images (single-shot spin-echo echo-planar sequence, with twice-refocused balanced diffusion-encoding gradients (*15*); 2 × 64 diffusion-encoding directions, 2-mm isotropic voxel size; 63 slices; *b*-value [degree of diffusion weighting] = 1,000 s/mm^2; echo time, 121 ms; repetition time, 11.1 s; and generalized autocalibrating partial parallel acquisition reconstruction) were acquired on a 3-T Siemens Trio Scanner.

DTI datasets were processed using in-house MINC suite tools (McConnell Brain Imaging Centre, Montreal Neurologic Institute, McGill University, http://www2.bic.mni.mcgill.ca/). Datasets were motion-corrected and realigned to the T1-weighted anatomic scan using a mutual information-based algorithm (*16*). Mean diffusivity, FA, eigenvectors, and eigenvalues of the diffusion tensor were then calculated at each voxel of the 4-dimensional image. Fiber tracking was performed by the FACT (fiber assignment using a continuous-tracking algorithm) (*17*). The tracking was stopped if the FA was less than 0.2 or the curvature from one voxel to the next was greater than 40°. Only tracts that passed through the 2 tract–delineating volumes of interest (VOIs) in each hemisphere were retained. In the non-PT and control groups, the posterior limb of the internal capsule and cerebral peduncle were used. Because the internal capsule was affected in most of the PT group patients, the infarct region itself was used as a VOI in the affected hemisphere. For unaffected hemisphere regions of interest in the PT group, infarct regions were mirrored from the affected side.

The fractional anisotropy ratio (R_{FA}) was calculated as a ratio of the affected and unaffected hemisphere FA in the PT and non-PT groups and as left–right hemisphere R_{FA}s in the control group. In the PT group, tracts were subdivided into anterograde (i.e., below the stroke) and retrograde (i.e., above the stroke) portions relative to the lesion site.

PET

(*R*)-^{11}C-PK11195 was synthesized from its precursor (*R*)-*N*-desmethyl-PK11195 (ABX) according to the method of Camsonne et al. (*18*), yielding 2.59–2.96 GBq (70–80 mCi) (18%–20% radiochemical yield) of the final sterile product. The specific activity was in the range of 18.5–22.2 TBq/mmol (500–600 Ci/mmol). PET scans were obtained on a Siemens ECAT HR + scanner in 3-dimensional (3D) mode (resolution at 1 cm from center, 4.4-mm radial, 5.1-mm axial). Patients were injected with 550 MBq of (*R*)-^{11}C-PK11195 into an antecubital vein after a 10-min transmission scan. Dynamic emission data were acquired over 60 min (*19*). A filtered backprojection algorithm, supplied by the manufacturer, with a Hanning filter cutoff frequency of 0.4 cycles per pixel was used for reconstruction. After correction for scatter, attenuation, and random coincidences, an image volume comprising 21 frames with matrix dimensions of 128 × 128 × 63 voxels and a voxel size of 2.06 × 2.06 × 2.43 mm was obtained.

PET data analysis was performed in VINCI (version 2.55; Max Planck Institute for Neurological Research). Individual PET data were coregistered to the T1-weighted MR images (*20*), and fiber tract images were overlaid onto the anatomic MR images. Because tractography identifies only the remaining intact fibers on the affected side, tracts were significantly smaller on the affected side in the PT group. Thus, we did not use the tracts themselves for the analysis but placed a standard set of elliptic 3D VOIs along both PTs, manually adjusted these VOIs to the individual size of the brain stem (comprising 1 VOI for pons and 1 for mid brain) and semioval center on the unaffected side, and copied the VOIs to the affected tract. This procedure ensured that nearly identically sized VOIs were used on both sides, despite smaller residual tracts on the affected side. These standard VOIs would extend about 2 mm beyond the outlined tract to cover the entire cerebral peduncle and thus also include tracer uptake in the immediate surroundings of the tract (Fig. 1). One further ellipsoid region was placed in the infarct and mirrored about the interhemispheric fissure to obtain the counterpart region in the unaffected hemisphere. In patients with TIA the infarct regions were placed in the basal ganglia at the level of the internal capsule.

Uptake ratios (URs) between corresponding VOIs (affected side divided by unaffected side) were calculated from an average image of the last 40 min. Ratios greater than 1 indicate higher uptake on the affected side. These URs were compared within and between groups using 2-way ANOVA with the Student–Newman–Keuls (SNK) statistic for posthoc analysis at a corrected type I error level of 0.05. The use of 1 average image of the last 40 min for analysis was possible because the URs of averaged time–activity curves (time–activity curve for the affected side divided by time–activity curve for the unaffected side) were stable for a low- (semioval center) and high-affinity (infarct) VOI at 20 min after injection.

FIGURE 1. Placement of standardized 3D ellipsoid VOIs along tracings of PT derived from diffusion tensor images. VOI for brain stem (BS) consists of 2 ellipsoids for mid brain and pons. One 3D ellipsoid was used for semioval center (OC).

Within- and between-group differences were tested using repeated-measures ANOVA as appropriate, corrected for multiple comparisons (SNK statistic, $P = 0.01$ corrected). Linear regression analysis was performed between R_{FA} values and URs in the brain stem and infarct. Initial URs correlated with clinical outcome using Pearson product moment correlation.

RESULTS

Regional ^{11}C-PK1195 Uptake

The tracer UR in the infarct (UR_{inf}) was significantly increased at the initial measurement in both the PT and the non-PT groups, as compared with the control group ($P < 0.01$), with no difference between these 2 patient groups. During the follow-up period, tracer uptake decreased significantly in both patient groups and was no longer different from that of the control group (2-way repeated-measures ANOVA, SNK test for multiple comparisons; Fig. 2). Tracer uptake along the PT was increased in the PT group but not in the non-PT and control groups and only distal to the lesion (UR at the level of the brain stem [$UR_{brain\ stem}$]), indicating that remote AMG activity is specific for the affected PT below the infarct (Fig. 3A; 2-way ANOVA $P < 0.01$ corrected)). This considerable anterograde increase persisted over the 6-mo period (Fig. 3B; ANOVA, $P < 0.01$ corrected) and was not significantly different from the initial measurement (2-way repeated-measures ANOVA, $P > 0.05$). No changes were observed in retrograde tract portions (semioval center).

Differences in URs were also reflected in absolute activity concentration differences in Bq/cm^3 between VOIs on the affected side and VOIs on the unaffected side (data not shown).

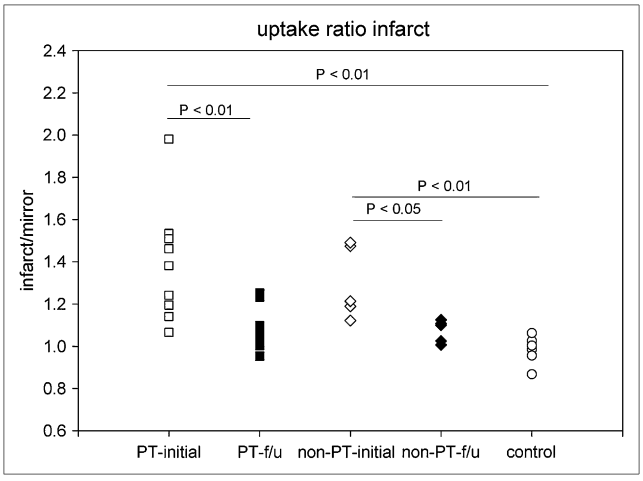

FIGURE 2. Tracer UR_{inf} in patients in whom the PT was affected (PT) and PT was not affected (non-PT) by stroke, compared with UR at level of internal capsule in controls. Ratios were increased in both patient groups initially and decreased over 6-mo follow-up (f/u) period (2-way repeated-measures ANOVA, SNK statistic for multiple comparisons).

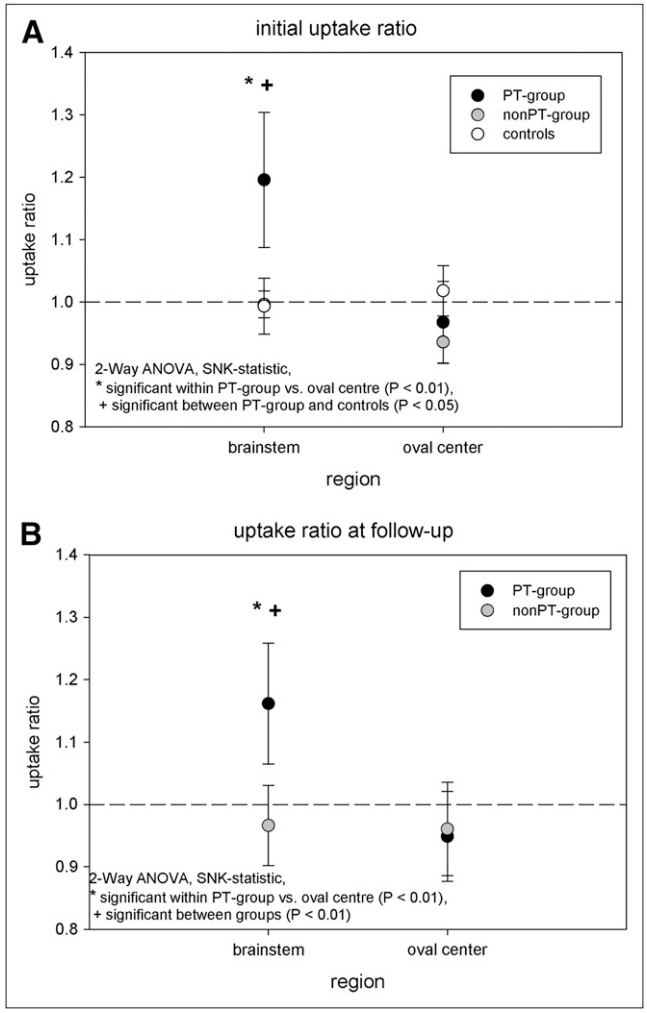

FIGURE 3. Tracer URs along PT in PT group, compared with non-PT group. URs are significantly higher in brain stem along affected tract below infarct initially (A) and at follow-up (B), whereas no increase is observed in semioval center, above infarct.

PT Damage and Correlation with ^{11}C-PK11195 Uptake

The R_{FA} was lower for the entire tract (total R_{FA}) and for the tract portions above (retrograde) and below ($R_{FA\text{-}below}$, anterograde) the infarct in the PT group, as compared with the non-PT group and controls at both times, thus indicating permanent tract damage in the PT group (2-way repeated-measures ANOVA, SNK statistic, $P < 0.01$). No significant change in R_{FA} was observed over time (Table 1).

At the initial measurement, the $UR_{brain\ stem}$ for ^{11}C-PK11195 was significantly negatively correlated with $R_{FA\text{-}below}$ ($r = -0.70$, $P = 0.019$; Fig. 4), indicating higher microglial activation with increasing tract damage (decreasing $R_{FA\text{-}below}$). A similar relationship was found for the follow-up measurement ($r = -0.72$, $P = 0.012$; Fig. 4).

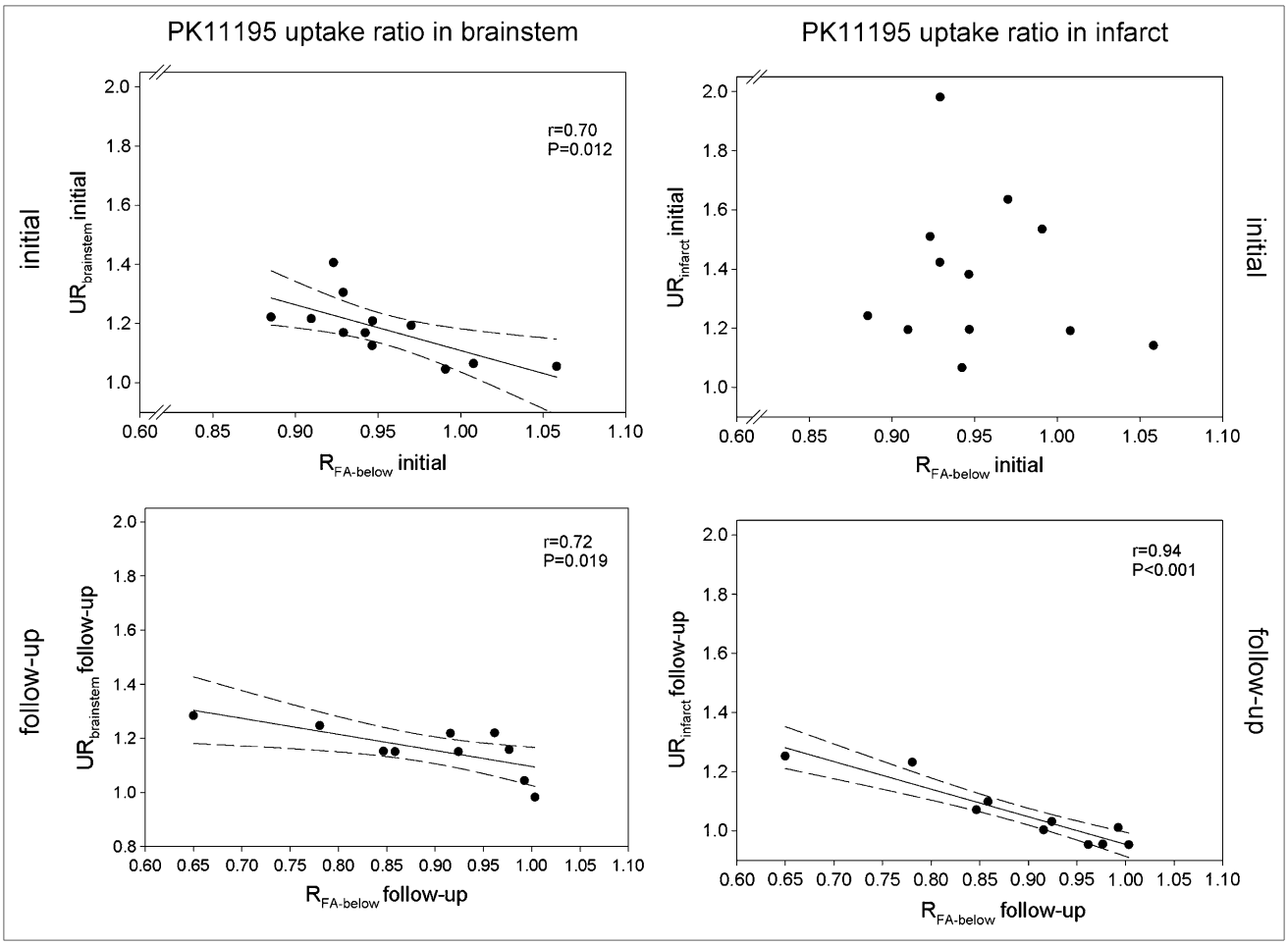

FIGURE 4. Correlation between tracer UR_{inf} and $UR_{brain\ stem}$ and anterograde fiber tract damage ($R_{FA\text{-}below}$). Extent of microglial activation correlated with tract damage only at follow-up, whereas AMG in brain stem related to anterograde fiber tract damage at both times.

There was no significant relationship between tracer UR_{inf} and tract damage (either entire tract or any of its portions) for the initial measurements. At follow-up, however, a highly significant correlation between persisting UR_{inf} and $R_{FA\text{-}below}$ was found ($r = -0.92$, $P < 0.01$; Figs. 4 and 5).

Correlation of Initial Parameters with Clinical Outcome

Motor function as measured by the RMFT was initially more impaired in patients in the PT group (rank sum test, $P = 0.041$) than in the non-PT group. PT group patients had significantly higher RMFT scores at follow-up than initially (Wilcoxon test, $P = 0.047$); no significant change was observed in the non-PT group. In the PT group, initial tract total R_{FA} correlated significantly with initial RMFT ($r = 0.92$, $P < 0.001$), and follow-up total R_{FA} correlated significantly with RMFT scores at follow-up ($r = 0.78$, $P = 0.012$).

To further investigate the impact of initial local and remote AMG on outcome, we correlated initial UR_{inf} and $UR_{brain\ stem}$ with RMFT at follow-up. No correlation was found between initial $UR_{brain\ stem}$ and motor function. When controlling for permanent tract damage (total R_{FA} at follow-up) using partial correlation, the initial $UR_{brain\ stem}$ showed a significant positive correlation with follow-up RMFT score ($\rho = 0.67$, $P = 0.035$). The initial UR_{inf} had a trend toward a negative association with motor outcome ($r = -0.63$, $P = 0.053$). This trend persisted when controlling for permanent tract damage (total R_{FA} at follow-up) using partial correlation ($\rho = -0.62$, $P = 0.052$).

DISCUSSION

This is the first—to our knowledge—prospective, controlled longitudinal study describing the temporal dynamics of AMG and its relationship to morphologic PT damage in humans with subcortical stroke using ^{11}C-PK11195 PET and DTI. Although microglial activity in the infarct decreases during recovery, remote activity in the brain stem along the affected tract persists. Microglial activation in general seems to be related only to anterograde PT damage but again with different temporal dynamics: in the brain

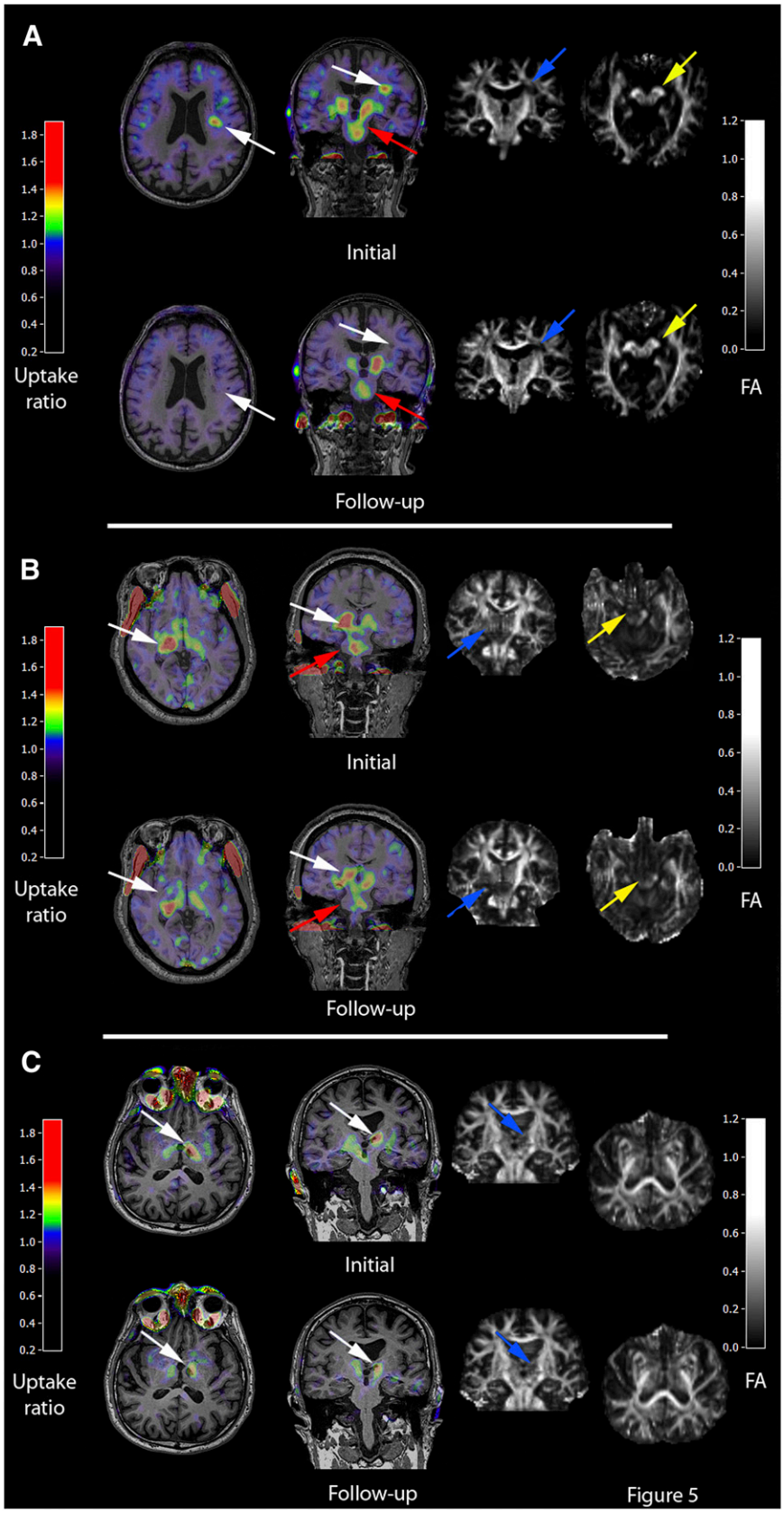

FIGURE 5. (A) Microglial activation in patient with small subcortical infarct and good recovery. Initial activated microglia in infarct decreased over 6 mo (white arrows), whereas microglial activation in brain stem persisted (red arrows). DTI showed decreased FA primarily in infarct (blue arrows) and less along tract at level of cerebral peduncles (yellow arrows). (B) Patient with complete transection of PT and poor recovery. Microglial activity in infarct decreased but still persisted after 6 mo (white arrows), as did activity in brain stem (red arrows). FA decreased in area of infarct (blue arrows) and along tract in cerebral peduncle (yellow arrows). Microglial activity in patient in whom PT was not affected (C) decreased over 6 mo (white arrows). No tracer uptake at level of brain stem was observed, and FA along tracts was not decreased.

stem, remote AMG related to PT damage during the entire observation period, whereas microglial activity in the infarct related to PT damage only after 6 mo.

Does ^{11}C-PK11195 Measure Microglial Activity in Stroke?

^{11}C-PK11195 has been widely used for imaging of AMG during the past 20 y (*21*). Early studies in animal models of ischemic stroke, using autoradiography in combination with immunostaining for macrophage cell lines, demonstrated that the ^{11}C-PK11195 signal associated with ischemic lesions originated primarily from macrophages (*22*). A more recent immunohistochemical study using antibodies that directly bind to the TSPO receptor in postmortem human brains confirmed that the expression of TSPO in the normal brain is minimal and that microglia and macrophages are the primary cell types exhibiting an increased number of TSPO binding sites in human pathologies (*8*). Astrocytes can also express TSPO in degenerative disease models (*23*) or in the infarct, where they contribute to scar formation. A recent small-animal PET study in rats using a new TSPO ligand directly compared immunohistology with imaging data and found that microglial and not astrocyte migration best correlated with the time course of tracer uptake. The authors concluded that either expression of TSPO is higher in microglia than in astrocytes, even at late times after ischemia, or different glial cell types express different TSPO subtypes (*24*). The contribution of astrocytes to the PET signal thus awaits further clarification.

Although there are some limitations to the use of ^{11}C-PK11195 as a radiotracer for microglia imaging (signal-to-noise ratio, unspecific binding), the most promising alternatives (*25*) have so far been tested only in a few healthy subjects (*26,27*), so the use of these alternative radiotracers in ischemia or other brain pathologies has not yet been established. In this study, we addressed the limitations of ^{11}C-PK11195 in 2 ways. First, given the specific hypotheses (increase of tracer uptake along the PT in the brain stem and semioval center), we have chosen a VOI approach, which is more robust to fluctuations in signal-to-noise ratio. Second, we used URs relative to mirrored regions in the unaffected hemisphere to avoid the use of a single reference region, thus accounting for a possible varying tracer binding in the unaffected hemisphere. Even if there were some unspecific binding in those mirrored regions, it would only bias our results in a conservative direction.

AMG in Infarct

The time course and cellular physiology of AMG in ischemia has been extensively studied in animal models of stroke. About 3–5 d after 1 h of transient focal ischemia, microglial activity has been found to peak in and around the area of the infarct in a mouse model, persisting at relatively high levels (*28*). In a recent imaging study using a new TSPO receptor ligand with a 2-h transient focal ischemia model in rats, peak activities were observed after 9–11 d (*24*). Local AMG can produce toxic substances that may ultimately promote delayed death of neurons around the infarct (*29*). However, AMG around the infarct may also be indirectly neuroprotective by neutralizing the effect of neutrophils (*30*) and removing debris from the infarct site (*5*). More recently, it has been demonstrated that AMG can also produce BDNF (brain-derived neurotrophic factor) (*31*) and thus actively contribute to neuronal regeneration.

Previous case series with ^{11}C-PK11195 PET in human stroke showed results comparable to those of animal studies with respect to the early occurrence of the microglial response (~day 3), which persisted in some subjects up to 150 d (*32*). The specificity of those findings, however, remained unclear because of the lack of controls. In our study, an early increase (3 d in the earliest of our patients) was observed in the infarct region of all stroke patients. The initial presence of AMG appeared to be a more-or-less stereotyped reaction and was not significantly different between the PT group and non-PT groups. This observation is in line with a recent ^{11}C-PK11195 study in a rat model of permanent ischemia, in which the extent of microglial activation also was independent of infarct location or size (*33*).

Over the 6-mo follow-up period, the UR decreased in all stroke patients. Although on average this activity was no longer significantly different from that in the controls, some variability of ^{11}C-PK11195 URs in the infarct remained (Fig. 2). Data from animal experiments on such extended periods are limited. In a recent study in rats, Keiner et al. also described a decrease of microglial activity in the perilesional zone at 42 d after permanent photothrombotic ischemia (*34*).

Remote AMG

In contrast to the infarct region, ^{11}C-PK11195 URs in the brain stem were significantly increased initially and at follow-up but only in those patients in whom the PT was affected by the stroke (Fig. 3). These results expand on previous observations from uncontrolled case series (*35*), because they demonstrate that increased URs in the brain stem are indeed specific for the damaged tract and not an unspecific reaction to the ischemic event per se. Our results suggest that this increased remote uptake has temporal dynamics different from AMG at the infarct site. Remote microglial activity has previously been described in animal models to occur around day 2 after the infarct and maximize around 7 d after ischemia (*6*). However, in single case studies of human stroke, ipsilesional thalamic ^{11}C-PK11195 binding was detected several months after the event (*35*). In our study, the URs at follow-up were not significantly different from initial URs, thus indicating that microglial activity along the damaged tract is relatively constant over the 6-mo follow-up period. Some tracer uptake was also observed in the unaffected hemisphere (e.g., the thalamus in Fig. 5). This uptake may correspond to an increased level of inflammation related to microangiopathy secondary to diabetes, hypertension, or age (*36*). Larger studies with stratification of risk factors and a tracer

with less unspecific binding than PK11195 are needed to verify this observation. These results again support the choice of TIA patients as controls; these TIA patients were comparable to the patient group with respect to these factors.

Relationship to Fiber Tract Damage

FA measurements of fiber tracts are generally regarded as an indicator of tract damage (*37*). We have shown that R_{FA}s within the first weeks correlate with clinical stroke severity and outcome after 6 mo. This finding seems to indicate that initial R_{FA}s are a good indicator of the extent of acute and long-term ischemic damage. A decrease in FA distal to the lesion after the first few weeks has been described by some authors (*12*) and interpreted as a correlate of Wallerian degeneration (*38*). We found a significantly lower R_{FA} initially and at follow-up for the entire tract and for the tract portions above and below the infarct. ^{11}C-PK11195 uptake, whether locally in the infarct or remotely in the brain stem, related to fiber tract damage in only the portion below the infarct. Again, remote and local AMG show a different association to tract damage: although remote AMG related to $R_{FA\text{-}below}$ initially and at follow-up, AMG in the infarct was highly correlated with $R_{FA\text{-}below}$ only after 6 mo (Fig. 4). This result suggests that the extent of acute (mostly ischemic) damage to the tract in the first days after the stroke determines the intensity of remote, anterograde microglial activation and may thus be related to the amount of axonal damage that will eventually lead to Wallerian degeneration. This interpretation is in line with data from an animal study in focal intracerebral hemorrhage (*39*).

In contrast, AMG in the infarct at the initial measurement is not related to anterograde tract damage per se. Only over time, when degeneration sets in (which is reflected by the $R_{FA\text{-}below}$ at follow-up), does persisting AMG significantly correlate with anterograde tract damage. Although AMG in the infarct decreases over time on average (Fig. 2), there are still patients with increased URs 6 mo after the ischemia. In those patients, persistent activity seems to have caused more anterograde degeneration.

The 2 patients in Figure 5 illustrate persistent activity. A patient with partial damage to the PT (Fig. 5A) exhibits microglial activation in the infarct, which vanishes over time. Damage to the tract is mainly limited to the area of the infarct in the corresponding FA image; the tract itself is less affected. In contrast, AMG persists in a patient with complete transection of the PT at the level of the internal capsule (Fig. 5B) and poor outcome. Here the FA image already shows tract damage at the level of the brain stem. In both patients, remote AMG is found at both times. No AMG is observed in the brain stem of a patient in whom the PT is not affected (Fig. 5C).

AMG and Clinical Outcome

The question of whether increased AMG activity is beneficial or detrimental to poststroke recovery remains unanswered (*40*). A recent stroke-recovery study in rodents observed better outcome in animals with lower AMG activity in the periinfarct zone (*34*). To explore these relationships further, we asked the question of whether measurement of local or remote AMG early after stroke might provide any additional information on stroke outcome beyond that already obtained through FA measurement. We thus performed a partial correlation analysis between initial URs and clinical outcome after 6 mo while controlling for damage to the entire tract as measured with R_{FA}. Interestingly, there was a trend toward a negative partial correlation between initial microglial activity in the infarct and outcome as assessed with the RMFT, whereas remote AMG was positively correlated with outcome. The results of this exploratory analysis may suggest that beyond ischemic tract damage initial microglial activation in the area of the infarct might influence outcome negatively, and initial remote AMG might be regarded as a positive influence. However, the relative impact of each of these processes and their exact role for stroke recovery remain to be determined.

CONCLUSION

The results of this study provide the first, to our knowledge, in vivo evidence for a relationship between microglial activity and fiber tract integrity in human subcortical stroke. We demonstrated that periinfarct and remote microglial activity not only follow different time courses during a 6-mo period after subcortical stroke but also are differentially related to anterograde fiber tract damage and might contribute differently to clinical outcome. In vivo microglia imaging combining PET and DTI may thus prove useful in the assessment of complex interrelationships between neuronal damage and poststroke neuroinflammation and provide surrogate markers for testing therapeutic strategies to modulate microglial activity toward favorable recovery at the transition from animal experiments to clinical trials.

ACKNOWLEDGMENTS

We thank Sharon Shapiro, Catherine Forbes, and the stroke team of the SMBD Jewish General Hospital for their enthusiastic support, and we thank the Cyclotron Unit of the McConnell Brain Imaging Centre. This study was supported by a Canadian Institute for Health Research operating grant ("The Neurobiology of Post-Stroke Recovery"), Canada Foundation for Innovation leader opportunity fund, and the Fondation pour la recherche en santé de Quebec.

REFERENCES

1. Wang X, Feuerstein GZ. The Janus face of inflammation in ischemic brain injury. *Acta Neurochir Suppl (Wien).* 2004;89:49–54.
2. Kreutzberg GW. Microglia: a sensor for pathological events in the CNS. *Trends Neurosci.* 1996;19:312–318.
3. Myers R, Manjil LG, Frackowiak RS, Cremer JE. [^{3}H]PK 11195 and the localisation of secondary thalamic lesions following focal ischaemia in rat motor cortex. *Neurosci Lett.* 1991;133:20–24.

4. Schroeter M, Jander S, Witte OW, Stoll G. Heterogeneity of the microglial response in photochemically induced focal ischemia of the rat cerebral cortex. *Neuroscience.* 1999;89:1367–1377.
5. Stoll G, Jander S, Schroeter M. Inflammation and glial responses in ischemic brain lesions. *Prog Neurobiol.* 1998;56:149–171.
6. Morioka T, Kalehua AN, Streit WJ. Characterization of microglial reaction after middle cerebral artery occlusion in rat brain. *J Comp Neurol.* 1993;327:123–132.
7. Block F, Dihne M, Loos M. Inflammation in areas of remote changes following focal brain lesion. *Prog Neurobiol.* 2005;75:342–365.
8. Cosenza-Nashat M, Zhao ML, Suh HS, et al. Expression of the translocator protein of 18 kDa by microglia, macrophages and astrocytes based on immunohistochemical localization in abnormal human brain. *Neuropathol Appl Neurobiol*. 2009;35:306–328.
9. Anholt RR, Pedersen PL, De Souza EB, Snyder SH. The peripheral-type benzodiazepine receptor: localization to the mitochondrial outer membrane. *J Biol Chem.* 1986;261:576–583.
10. Benavides J, Quarteronet D, Imbault F, et al. Labelling of "peripheral-type" benzodiazepine binding sites in the rat brain by using [^{3}H]PK 11195, an isoquinoline carboxamide derivative: kinetic studies and autoradiographic localization. *J Neurochem.* 1983;41:1744–1750.
11. Radlinska BA, Ghinani SA, Lyon P, et al. Multimodal microglia imaging of fiber tracts in acute subcortical stroke. *Ann Neurol.* 2009;66:825–832.
12. Liang Z, Zeng J, Liu S, et al. A prospective study of secondary degeneration following subcortical infarction using diffusion tensor imaging. *J Neurol Neurosurg Psychiatry.* 2007;78:581–586.
13. Mukherjee P. Diffusion tensor imaging and fiber tractography in acute stroke. *Neuroimaging Clin N Am.* 2005;15:655–665.
14. Lincoln N, Leadbitter D. Assessment of motor function in stroke patients. *Physiotherapy.* 1979;65:48–51.
15. Reese TG, Heid O, Weisskoff RM, Wedeen VJ. Reduction of eddy-current-induced distortion in diffusion MRI using a twice-refocused spin echo. *Magn Reson Med.* 2003;49:177–182.
16. Maes F, Collignon A, Vandermeulen D, Marchal G, Suetens P. Multimodality image registration by maximization of mutual information. *IEEE Trans Med Imaging.* 1997;16:187–198.
17. Mori S, Crain BJ, Chacko VP, van Zijl PCM. Three-dimensional tracking of axonal projections in the brain by magnetic resonance imaging. *Ann Neurol.* 1999;45:265–269.
18. Camsonne R, Crouzel C, Comar D, et al. Synthesis of *N*-(^{11}C) methyl, *N*-(methyl-1 propyl), (chloro-2 phenyl)-1 isoquinoleine carboxamide-3 (Pk 11195): a new ligand for peripheral benzodiazepine receptors. *J Labelled Comp Radiopharm.* 1984;21:985–991.
19. Kropholler MA, Boellaard R, Schuitemaker A, et al. Development of a tracer kinetic plasma input model for (*R*)-[^{11}C]PK11195 brain studies. *J Cereb Blood Flow Metab.* 2005;25:842–851.
20. Cizek J, Herholz K, Vollmar S, Schrader R, Klein J, Heiss WD. Fast and robust registration of PET and MR images of human brain. *Neuroimage.* 2004;22:434–442.
21. Hashimoto K, Inoue O, Suzuki K, Yamasaki T, Kojima M. Synthesis and evaluation of ^{11}C-PK 11195 for in vivo study of peripheral-type benzodiazepine receptors using positron emission tomography. *Ann Nucl Med.* 1989;3:63–71.
22. Myers R, Manjil LG, Cullen BM, Price GW, Frackowiak RS, Cremer JE. Macrophage and astrocyte populations in relation to [^{3}H]PK 11195 binding in rat cerebral cortex following a local ischaemic lesion. *J Cereb Blood Flow Metab.* 1991;11:314–322.
23. Ji B, Maeda J, Sawada M, et al. Imaging of peripheral benzodiazepine receptor expression as biomarkers of detrimental versus beneficial glial responses in mouse models of Alzheimer's and other CNS pathologies. *J Neurosci.* 2008; 28:12255–12267.
24. Martin A, Boisgard R, Theze B, et al. Evaluation of the PBR/TSPO radioligand [^{18}F]DPA-714 in a rat model of focal cerebral ischemia. *J Cereb Blood Flow Metab.* 2010;30:230–241.
25. Chauveau F, Boutin H, Van CN, Dolle F, Tavitian B. Nuclear imaging of neuroinflammation: a comprehensive review of [^{11}C]PK11195 challengers. *Eur J Nucl Med Mol Imaging.* 2008;35:2304–2319.
26. Fujimura Y, Kimura Y, Simeon FG, et al. Biodistribution and radiation dosimetry in humans of a new PET ligand, ^{18}F-PBR06, to image translocator protein (18 kDa). *J Nucl Med.* 2010;51:145–149.
27. Kreisl WC, Fujita M, Fujimura Y, et al. Comparison of [^{11}C]-(*R*)-PK 11195 and [^{11}C]PBR28, two radioligands for translocator protein (18 kDa) in human and monkey: Implications for positron emission tomographic imaging of this inflammation biomarker. *Neuroimage.* 2009;49:2924–2932.
28. Gelderblom M, Leypoldt F, Steinbach K, et al. Temporal and spatial dynamics of cerebral immune cell accumulation in stroke. *Stroke.* 2009;40: 1849–1857.
29. Kaushal V, Schlichter LC. Mechanisms of microglia-mediated neurotoxicity in a new model of the stroke penumbra. *J Neurosci.* 2008;28:2221–2230.
30. Neumann J, Sauerzweig S, Ronicke R, et al. Microglia cells protect neurons by direct engulfment of invading neutrophil granulocytes: a new mechanism of CNS immune privilege. *J Neurosci.* 2008;28:5965–5975.
31. Madinier A, Bertrand N, Mossiat C, et al. Microglial involvement in neuroplastic changes following focal brain ischemia in rats. *PLoS ONE.* 2009;4:e8101.
32. Gerhard A, Schwarz J, Myers R, Wise R, Banati RB. Evolution of microglial activation in patients after ischemic stroke: a [^{11}C](*R*)-PK11195 PET study. *Neuroimage.* 2005;24:591–595.
33. Schroeter M, Dennin MA, Walberer M, et al. Neuroinflammation extends brain tissue at risk to vital peri-infarct tissue: a double tracer [^{11}C]PK1. *J Cereb Blood Flow Metab.* 2009;29:1216–1225.
34. Keiner S, Wurm F, Kunze A, Witte OW, Redecker C. Rehabilitative therapies differentially alter proliferation and survival of glial cell populations in the perilesional zone of cortical infarcts. *Glia.* 2008;56:516–527.
35. Pappata S, Levasseur M, Gunn RN, et al. Thalamic microglial activation in ischemic stroke detected in vivo by PET and [^{11}C]PK1195. *Neurology.* 2000;55:1052–1054.
36. Popa-Wagner A, Badan I, Vintilescu R, Walker L, Kessler C. Premature cellular proliferation following cortical infarct in aged rats. *Rom J Morphol Embryol.* 2006;47:215–228.
37. Moller M, Frandsen J, Andersen G, Gjedde A, Vestergaard-Poulsen P, Ostergaard L. Dynamic changes in corticospinal tracts after stroke detected by fibretracking. *J Neurol Neurosurg Psychiatry.* 2007;78:587–592.
38. Thomalla G, Glauche V, Koch MA, Beaulieu C, Weiller C, Rother J. Diffusion tensor imaging detects early Wallerian degeneration of the pyramidal tract after ischemic stroke. *Neuroimage.* 2004;22:1767–1774.
39. Wasserman JK, Schlichter LC. White matter injury in young and aged rats after intracerebral hemorrhage. *Exp Neurol.* 2008;214:266–275.
40. Lai AY, Todd KG. Microglia in cerebral ischemia: molecular actions and interactions. *Can J Physiol Pharmacol.* 2006;84:49–59.